Criticality Computation with Finite Element Method on Non-Conforming Meshes

L. Giret, Jr. Ciarlet P, E. Jamelot

M&C 2017 - International Conference on Mathematics & Computational Methods Applied to Nuclear Science & Engineering, Jeju, Korea, April 16-20, 2017, on USB (2017)

Criticality Computation with Finite Element Method on Non-Conforming Meshes

Léandre Giret,* Patrick Ciarlet,† Erell Jamelot*

*Commissariat à l'Énergie Atomique et aux Énergies Alternatives, CEA-Saclay, DEN/DANS/DM2S/SERMA/LLPR, 91191 Gif-sur-Yvette, France

†POEMS Laboratory, CNRS-INRIA-ENSTA UMR 7231, ENSTA Paristech, 828 Boulevard des Maréchaux, 91120 Palaiseau, France

leandre.giret@cea.fr, patrick.ciarlet@ensta-paristech.fr, erell.jamelot@cea.fr

Abstract - *In this work, we proposed and study a method to use non-conforming meshing for core reactor simulation. This consists in a domain decomposition with Lagrange multipliers of the well known Raviart-Thomas finite element method. Here, we provide an a priori error estimate for criticality computation.*

I. INTRODUCTION

The steady state of a nuclear reactor is characterised by its criticality. In order to compute this value one has to solve a generalised eigenvalue problem. From the Krein-Rutman [1] theorem we know that the only physical solution is the eigenfunction associated with the smallest eigenvalue (the fundamental mode). The usual way to compute this solution is to use the inverse power iteration, which consists in solving a source problem generated by the solution from the previous iterations.

APOLLO3® is a common neutronic platform of CEA and EDF. It includes different deterministic solvers. We present here a new development in the MINOS solver [2] which is based on the Raviart-Thomas-Nédélec (or RTN) finite element method (or FEM) for Cartesian and hexagonal grids and includes a domain decomposition method (or DDM). The method currently implemented is an optimised Schwarz DDM [3, 4, 5].

The macroscopic cross sections used to solve the SP_N equations are homogenised assembly by assembly or cell by cell. Therefore the cross sections are modelled separately on each materials, thus where three or more materials intersect the solution can be of low-regularity [6]. The low-regularity of a function can be interpreted as a function with a non-smooth gradient. The areas where the solution is no more regular are called singularities. To obtain a better estimate of the solution, one can refine the mesh where the singularities occur. Refining a Cartesian grid quickly increases the number of degrees of freedom. Thus, it is interesting to use a DDM with local conforming grids but non-conforming meshes at the interfaces. To do that, we use a DDM with Lagrange multipliers [7, 8] which is algebraically equivalent to the Schur complement method.

Moreover, this adaptation helps for modelling Cartesian plate reactors and fast neutron reactors. Indeed, these reactors have non-conforming geometry and to mesh them one has to extrude lines all over the geometry of the reactor. The resulting number of cells can be reduced by meshing each assembly independently. For instance in Figure 1, one can notice that the non-conforming mesh contains nearly half cells than the conforming one. This illustrate that non-conforming meshes can be used to reduce the memory usage of the solver.

To validate this method, one needs to do its numerical analysis. Indeed, this analysis proves that the method converges to the solution we are looking for. Moreover, a priori error estimations help to calibrate the solver and it is the first step to evaluate the propagation of uncertainties in it.

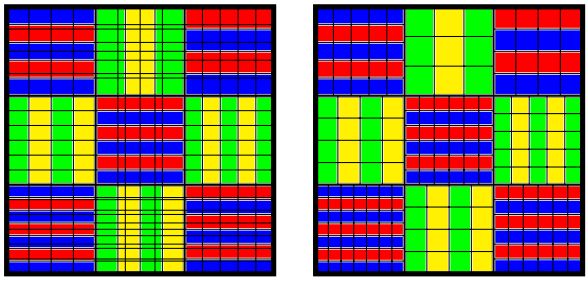

Fig. 1. Plate reactor conforming mesh (*left*) with 390 cells and non-conforming mesh (*right*) with 212 cells.

The functional framework of the numerical analysis is given by the so-called Sobolev's spaces. Those functional spaces generalised differentiability to functions in L^2 (square-integrable functions). Here, we use the following Sobolev's spaces, for a domain Ω in $\mathbb{R}^d$, $d = 2, 3$ and r a real in $]0, 1[$:

$$H^1(\Omega) = \left\{u \in L^2(\Omega), \boldsymbol{\nabla} u \in L^2(\Omega)\right\}$$

$$H^1_0(\Omega) = \left\{u \in H^1(\Omega),\, u|_{\partial\Omega} = 0\right\}$$

$$H^r(\Omega) = \left\{u \in L^2(\Omega),\, \iint_{\Omega\times\Omega} \frac{|u(x) - u(y)|^2}{\|x - y\|^{d+2r}} dxdy < \infty\right\}$$

The mathematical theory of the mixed problem discretisation was done for at least piecewise H^{1+r} solutions, with $r > 1/4$. H^{1+r} is the space of all functions in H^1 such that their gradients are in H^r. But as the cross sections are highly heterogeneous the solution is no more regular than $H^{1+r_{\max}}$ where $r_{\max}$ can be smaller than $1/4$ and depends on the geometry and the cross sections. The mathematical theory has then to be extended for both source and eigenvalue problems. This is the purpose of this paper for the following cases: the SP_1/diffusion equations without or with non-conforming DDM and the SP_N multigroup equations with DDM.

The outline of the paper is as follows: first we do the numerical analysis for the SP_1/diffusion equation, then we show how to extend it to the SP_N equations. Finally we present some realistic numerical results.

II. THE SP_1/DIFFUSION EQUATION

We denote the domain of the reactor by $\mathcal{R}$. $\mathcal{R}$ is supposed to be a bounded, connected and open subset of $\mathbb{R}^d$, $d = 2, 3$.b We choose to treat zero flux boundary condition but our work could be extended to other conditions (symmetry, reflexive. . .). The SP_1/diffusion equation reads:
Find $(\mathbf{p}, \phi, k_{\text{eff}})$ such that:

$$\left\{\begin{array}{rcll} D^{-1}\mathbf{p} + \mathbf{grad}\phi &=& 0 & \text{in } \mathcal{R}, \\ \text{div } \mathbf{p} + \Sigma_a\phi &=& \frac{1}{k_{\text{eff}}}\nu\Sigma_f\phi & \text{in } \mathcal{R}, \\ \phi|_{\partial\mathcal{R}} &=& 0 & \text{on } \partial\mathcal{R}. \end{array}\right. \tag{1}$$

Above, $\mathbf{p}$ represents the neutron current and ϕ the neutron scalar flux. We denote by Σ_s^0 (resp. Σ_s^1) the zero-th (resp. first) angular moment of the scattering cross section. If we let Σ_t be the total cross section, then $\Sigma_a = \Sigma_t - \Sigma_s^0$ is the absorption cross section. We have $D = (3\Sigma_t)^{-1}$ for the diffusion equation and $D = (3(\Sigma_t - \Sigma_s^1))^{-1}$ for the SP_1 equation. We recall that the cross sections and the diffusion coefficient are required to have only a piecewise regularity, for example to be piecewise polynomial.

1. Inverse Power Iteration

After some initial guess $(\mathbf{p}^0, \phi^0, k_{\text{eff}}^0)$ is provided, at iteration number $m+1$, we deduce $(\mathbf{p}^{m+1}, \phi^{m+1}, k_{\text{eff}}^{m+1})$ from $(\mathbf{p}^m, \phi^m, k_{\text{eff}}^m)$ by solving (1) with a source term. The inverse power iteration reads:

Set $(\mathbf{p}^0, \phi^0, k_{\text{eff}}^0)$, $m = 0$
Until convergence, do: $m \leftarrow m + 1$
Solve :

$$\left\{\begin{array}{rcl} D^{-1}\mathbf{p}^{m+1} + \mathbf{grad}\phi^{m+1} &=& 0 \\ \text{div } \mathbf{p}^{m+1} + \Sigma_a\phi^{m+1} &=& \frac{1}{k_{\text{eff}}^m}\nu\Sigma_f\phi^m \\ \phi|_{\partial\mathcal{R}}^{m+1} &=& 0 \end{array}\right. \tag{2}$$

Compute: $k_{\text{eff}}^{m+1} = k_{\text{eff}}^m \frac{\int_{\mathcal{R}}\left(\Sigma_f\phi^{m+1}\right)^2}{\int_{\mathcal{R}}\left(\Sigma_f\phi^{m+1}\Sigma_f\phi^m\right)^2}$

End

At each iteration the so-called source problem has to be solved with $(\mathbf{p}^{m+1}, \phi^{m+1})$ as unknowns. Let us study the RTN FEM on Cartesian grids.

2. Finite Element Method

From now on, let us consider the source problem (2) where we replace the left hand side of the problem (1) by S_f:

$$\left\{\begin{array}{rcll} D^{-1}\mathbf{p} + \mathbf{grad}\phi &=& 0 & \text{in } \mathcal{R}, \\ \text{div } \mathbf{p} + \Sigma_a\phi &=& S_f & \text{in } \mathcal{R}, \\ \phi &=& 0 & \text{on } \partial\mathcal{R}. \end{array}\right. \tag{3}$$

We recall that under additional mild assumptions on the parameters, the solution ϕ, for any source S_f in $L^2(\mathcal{R})$, has some extra regularity (see [8], Proposition 1). Indeed, if the cross sections are piecewise polynomial, thus there exists $r_{\max} > 0$ such that the solution ϕ is in $H^{1+r_{\max}}(\mathcal{R})$. From now on we suppose that $r_{\max}$ is less than $1/2$. This is the case for low-regular solutions.

We denote by $\mathbf{Q}$ the space of functions in $\left(L^2(\mathcal{R})\right)^d$ with their divergence in $L^2(\mathcal{R})$:$\mathbf{Q} = \mathbf{H}(\text{div }, \mathcal{R})$. The solution $(\mathbf{p}, \phi)$ is looked for in $\mathbf{X} = \mathbf{Q} \times L^2(\mathcal{R})$. The space $\boldsymbol{X}$ can be normed with

$$\|(\boldsymbol{p}, \phi)\|_{\boldsymbol{X}}^2 = \|\boldsymbol{p}\|_{\boldsymbol{Q}}^2 + \|\phi\|_{L^2}^2 \tag{4}$$

The system (3) can be written as a variational problem on $\mathbf{X}$:

$$\forall(\mathbf{q}, \psi) \in \mathbf{X}, \left\{\begin{array}{rcl} a(\mathbf{p}, \mathbf{q}) + b(\mathbf{q}, \phi) &=& 0, \\ b(\mathbf{p}, \psi) + t(\phi, \psi) &=& (S_f, \psi). \end{array}\right. \tag{5}$$

With:

- $a(\mathbf{p}, \mathbf{q}) = -\int_{\mathcal{R}} D^{-1}\mathbf{p} \cdot \mathbf{q}$
- $b(\mathbf{q}, \psi) = \int_{\mathcal{R}} \text{div } \mathbf{q}\psi$
- $t(\phi, \psi) = \int_{\mathcal{R}} \Sigma_a\phi\psi$

To simplify the notations, we use in the following another form of (5) given by

$$\forall(\boldsymbol{q}, \psi) \in \boldsymbol{X}, c((\boldsymbol{p}, \phi), (\boldsymbol{q}, \psi)) = (S_f, \psi). \tag{6}$$

where c is defined over $\boldsymbol{X} \times \boldsymbol{X}$ by

$$c((\boldsymbol{p}, \phi), (\boldsymbol{q}, \psi)) = a(\boldsymbol{p}, \boldsymbol{q}) + b(\boldsymbol{q}, \phi) + b(\boldsymbol{p}, \psi) + t(\phi, \psi). \tag{7}$$

With the help of an inf-sup condition on the bilinear form c, one can prove the well posedness of the continuous problem [9, 10, 5]. We recall that $(\boldsymbol{p},\phi)$ is the solution to (5) associated to the source term S_f. Taking $(\boldsymbol{q}, \psi) = (-\boldsymbol{p}, \frac{\phi}{2} + \frac{1}{2\Sigma_a}\text{div } \boldsymbol{p})$ in $\boldsymbol{X}$, one can find

$$\|(\boldsymbol{q}, \psi)\|_{\boldsymbol{X}} \lesssim \|(\boldsymbol{p}, \phi)\|_{\boldsymbol{X}}. \tag{8}$$

Apply (6) with $(\boldsymbol{q}, \psi)$, we find the following estimation

$$|c((\boldsymbol{p}, \phi), (\boldsymbol{q}, \psi))| \gtrsim \|(\boldsymbol{p}, \phi)\|_{\boldsymbol{X}}\|(\boldsymbol{q}, \psi)\|_{\boldsymbol{X}}. \tag{9}$$

One can easily conclude to the following in-sup condition, there exists a constant $\beta > 0$ which depends only on the geometry such that

$$\inf_{(\boldsymbol{p},\phi)} \sup_{(\boldsymbol{q},\psi)} |c((\boldsymbol{p}, \phi), (\boldsymbol{q}, \psi))| > \beta \tag{10}$$

Let set $\mathbf{Q}_h$ the space of discretisation of $\mathbf{Q}$ by RTN FEM [11, 12]. The space used to discrete the flux ϕ is L_h^k, which contains all the piecewise polynomials with a degree smaller than k over the mesh. The discrete variational problem over $\mathbf{X}_h = \mathbf{Q}_h \times L_h^k$ reads then:

$$\forall(\mathbf{q}_h, \psi_h) \in \mathbf{X}_h, \left\{\begin{array}{rcl} a(\mathbf{p}_h, \mathbf{q}_h) + b(\mathbf{q}_h, \phi_h) &=& 0, \\ b(\mathbf{p}_h, \psi_h) + t(\phi_h, \psi_h) &=& (S_f, \psi_h). \end{array}\right. \tag{11}$$

As we proved the well posedness of the continuous problem (6), we have the following inf-sup condition for the discrete problem, with $\beta_h > 0$ converging uniformly to 0 when h tends to 0,

$$\inf_{(\boldsymbol{p}_h,\phi_h)} \sup_{(\boldsymbol{q}_h,\psi_h)} |c((\boldsymbol{p}_h, \phi_h), (\boldsymbol{q}_h, \psi_h))| > \beta_h. \tag{12}$$

To obtain an error estimate, we suppose from now on that the source term S_f is in H^μ with μ lower than $r_{\max}$. This implies a better regularity on the current:

- $\boldsymbol{p} \in H(\mathrm{div}\,, \mathcal{R}) \cap H^{\mu}(\mathcal{R})$
- $\mathrm{div}\,\boldsymbol{p} \in H^{\mu}(\mathcal{R})$

According to first Strang's lemma [13] the error reads:

$$\|(\boldsymbol{p}, \phi) - (\boldsymbol{p}_h, \phi_h)\|_X \lesssim \inf_{(\boldsymbol{q}_h, \psi_h) \in \boldsymbol{X}_h} \|(\boldsymbol{p}, \phi) - (\boldsymbol{q}_h, \psi_h)\|_X. \quad (13)$$

Let us bound the different contributions in the right-hand side of (13) for some appropriately chosen discrete field $\mathfrak{u}_h = (\boldsymbol{q}_h, \psi_h)$. Recall that $\mathfrak{u} = (\boldsymbol{p}, \phi)$.

- Consider the following orthogonal projection operators $\Pi_0 : L^2(\mathcal{R}) \to L^2_h$. There exists C independent of h such that ([13], Proposition 1.135):

$$\forall \psi \in H^1(\mathcal{R}), \|\psi - \Pi_0(\psi)\|_{L^2(\mathcal{R})} \lesssim h\|\psi\|_{H^1(\mathcal{R})}. \quad (14)$$

- Let $\boldsymbol{q} \in H^r(\mathcal{R})$, such that $\mathrm{div}\,\boldsymbol{q} \in H^s(\mathcal{R})$, $0 < r, s < r_{\max}$ and $\boldsymbol{q}_R$ be its RTN interpolant [14]. Thus it stands ([14], Lemma 3.3):

$$\begin{aligned} \|\boldsymbol{q} - \boldsymbol{q}_R\|_{L^2(\mathcal{R})} &\lesssim (h^r|\boldsymbol{q}|_{H^r(\mathcal{R})} + h\|\mathrm{div}\,\boldsymbol{q}\|_{L^2(\mathcal{R})}), \\ \|\mathrm{div}\,(\boldsymbol{q} - \boldsymbol{q}_R)\|_{L^2(\mathcal{R})} &\lesssim h^s|\mathrm{div}\,q|_{H^s(\mathcal{R})}. \end{aligned} \quad (15)$$

Using (13) with (14)-(15), one can easily conclude that under the assumptions on the cross sections, it holds, with $r_{\max} < 1/2$:

$$\begin{aligned} &\forall \mu \in]0, r_{\max}[, \forall S_f H^{\mu}(\mathcal{R}), \\ &\|\mathfrak{u} - \mathfrak{u}_h\|_X \lesssim h^{\mu}\|S_f\|_{H^{\mu}(\mathcal{R})}. \end{aligned} \quad (16)$$

One can notice that the previous analysis can be extended to the case where $r_{\max}$ is in $[1/2, 1]$ and $\mu < r_{\max}$ (or $\mu \leq 1$ if $r_{\max} = 1$).

3. Aubin-Nitsche-type estimates

We recall also that we denote $(\boldsymbol{p}, \phi)$ (resp. $(\boldsymbol{p}_h, \phi_h)$) the solution of the continuous (resp. discrete) variational problem (5) (resp. (11)). To derive improved estimates on the error $\|\phi - \phi_h\|_{L^2(\mathcal{R})}$, we shall rely on the illuminating work of Falk-Osborn [15], which provides such an estimate for an RTN-discretisation in $H(\mathrm{div}\,, \mathcal{R}) \times L^2(\mathcal{R})$ of the diffusion equation with smooth solution.

We recall that for any $\boldsymbol{q}$ in $\boldsymbol{Q}$, its RTN-interpolant is denoted by q_R and satisfies for any ψ_h in L_h :

$$b(\boldsymbol{q} - \boldsymbol{q}_R, \psi_h) = 0 \quad (17)$$

We also need to introduce the adjoint problem associated to (5):
For $d \in L^2(\mathcal{R})$, find $(\boldsymbol{y}_d, \eta_d) \in \boldsymbol{X}$ such that $\forall (\boldsymbol{q}, \psi) \in \boldsymbol{X}$:

$$a(\boldsymbol{y}_d, \boldsymbol{q}) + b(\boldsymbol{q}, \eta_d) + b(\boldsymbol{y}_d, \psi) + t(\eta_d, \psi) = \int_{\mathcal{R}} d\psi. \quad (18)$$

Adapting the methodology of [15] as done in [16], using the adjoint problem (18), one can prove that, for any source S_f in $H^{\mu}(\mathcal{R})$, $\mu < r_{\max}$, we have the a priori error estimate:

$$\|\phi - \phi_h\|_{L^2(\mathcal{R})} \lesssim h^{2\mu}\|S_f\|_{H^{\mu}(\mathcal{R})} \quad (19)$$

This is the best convergence rate of the method for low regularity solutions. This illustrates the fact that using higher order near the singularities is not efficient in practice to estimate them. Indeed, the ratio is given by the regularity of the solution and not by the order of the finite elements.

4. Eigenvalue Problem

With the help of the previous analysis, we can do the numerical analysis of the FEM for the approximation of the eigenvalue problem. We first have to show the convergence of the method in the spirit of the Osborn's theory in [17]. Then we find a better rate of convergence by adapting the work of Boffi et al. in[18].

Let μ denote the regularity of the eigenfunction, i.e. $\phi \in H^{1+\mu}(\mathcal{R})$, and B_{μ} (resp. B^h_{μ}) the operator which associates to a source S_f the continuous (resp. discrete) scalar flux, $B_{\mu}S_f = \phi$ (resp. $B^h_{\mu}S_f = \phi_h$). To prove the convergence of the method, we only need to show the norm convergence of the operator B^h_{μ} to B_{μ} [17]. This convergence is enough since they are compact operators from $H^{\mu}(\mathcal{R})$ to itself. This condition is fulfilled thanks to the convergence of the source problem.

We then obtain a convergence rate in h^{μ}. Following the work of [18], we can enhance this rate. The idea is to restrict the operators on the eigenspace E. Considering operators on finite dimension spaces, the trick is to use the equivalence of all norms. We obtain a norm convergence on the eigenspace given by:

$$\|B_{\mu} - B^h_{\mu}\|_{\mathcal{L}(E)} \leq Ch^{2\mu} \quad (20)$$

Then we can conclude that the convergence rate of the first eigenvalue is at least 2μ.

5. Non-Conforming Meshes

As said above, the solution can be singular where three or more materials intersect. In this case the mesh must be refined to have a better approximation. Because we work in a code that already contains a conforming DDM, we decided to adapt it so that it supports non-conforming meshes between subdomains.

We take a partition $(\mathcal{R}_i)_{i=1}^N$ of the reactor $\mathcal{R}$, we denote by Γ_{ij} the interface between two subdomains $\mathcal{R}_i$ and $\mathcal{R}_j$. We define the interface Γ_S by

$$\Gamma_S = \bigcup_{i=1}^{N} \bigcup_{j=i+1}^{N} \Gamma_{ij}. \quad (21)$$

We denote ϕ_i (resp. $\mathbf{p}_i$ and $S_{f,i}$) the restriction of the flux ϕ (resp. the current $\mathbf{p}$ and the source S_f) onto the domain $\mathcal{R}_i$, ϕ_S the restriction of the flux ϕ over all the interfaces Γ_S. The jump jump of the current $\mathbf{p}$ on Γ_{ij} is defined by

$$[\mathbf{p} \cdot \mathbf{n}]_{ij} = \sum_{k=i,j} \boldsymbol{p}_k \cdot \boldsymbol{n}_k|_{\Gamma_{ij}}. \quad (22)$$

Problem (1) with the domain decomposition can be written as:

$$\begin{cases} D^{-1}\mathbf{p}^i + \mathbf{grad}\phi^i = 0 & \text{in } \mathcal{R}_i & \forall i, \\ \mathrm{div}\,\mathbf{p}^i + \Sigma_a\phi^i = S^i_f & \text{in } \mathcal{R}_i & \forall i, \\ \phi_i = \phi_S & \text{on } \partial\mathcal{R}_i \cap \Gamma_S & \forall i, \\ [\mathbf{p} \cdot \mathbf{n}] = 0 & \text{on } \Gamma_S. & \end{cases} \quad (23)$$

We present below an innovative approach to derive the variational formulation, the space of the current p is chosen to

be $\mathbf{Q} = \left\{\mathbf{q} \in \mathcal{PH}(\mathrm{div}, \mathcal{R}) | \, [\mathbf{p}\cdot\mathbf{n}] \in L^2(\Gamma_S)\right\}$, where $\mathcal{PH}(\mathrm{div}, \mathcal{R})$ is the space of the piecewise $\mathbf{H}(\mathrm{div}, \mathcal{R})$ functions. The flux ϕ is searched in $L^2(\mathcal{R})$. The last unknown ϕ_S is just searched in $L^2(\Gamma_S)$.

The variational formulation derived from (23) reads: Find $(\mathbf{p}, \phi, \phi_S) \in \mathbf{Q} \times L^2(\mathcal{R}) \times L^2(\Gamma_S)$ such that $\forall (\mathbf{q}, \psi, \psi_S) \in \mathbf{Q} \times L^2(\mathcal{R}) \times L^2(\Gamma_S)$:

$$\left\{\begin{array}{rcl} a(\mathbf{p},\mathbf{q}) + b(\mathbf{q},\phi) - l_S(\mathbf{q},\phi_S) &=& 0, \\ b(\mathbf{p},\psi) + t(\phi,\psi) &=& (S_f,\psi), \\ l_S(\mathbf{p},\psi_S) &=& 0. \end{array}\right. \tag{24}$$

with:

- $l_S(\mathbf{q},\psi_S) = \int_{\Gamma_S} [\mathbf{p}\cdot\mathbf{n}]\psi_S$

In standard approach, $\phi_S \in H^{\frac{1}{2}}(\Gamma_S)$ and the discrete of the resulting variational formulation are not conforming which leads to technical difficulties when one wants to derive error estimates. In (24), taking $\mathbf{p} \in \mathbf{Q}$ allows to derive a conforming discretisation since ϕ_S and ϕ_S^h belong to $L^2(\Gamma_S)$. Thus error estimates are derived from the inf-sup condition.

On each subdomain $\mathcal{R}_i$ the current is in $\mathbf{H}(\mathrm{div}, \mathcal{R}_i)$, so that $\mathbf{p}$ is discretised by local RTN elements. Thus each subdomain can be meshed separately by a Cartesian grid.

All the previous analysis holds true for (24) as done in [8, 16].

Then, it remains to mesh the interfaces between subdomains. To do that we can just take the intersection of the neighbouring subdomain meshes at the interface as shown in figure 2.

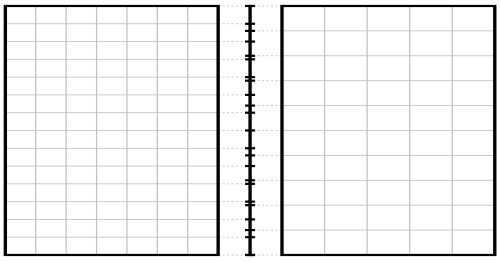

Fig. 2. Mesh of an interface between two subdomains with different mesh sizes.

The order of the elements used for the Lagrange multiplier is the same as the one used for the restriction of the current ($\mathbf{p}$) on the interface. For instance, with RT0 elements, ϕ_S is piecewise constant.

Another way to mesh the Lagrange multiplier ϕ_S is to use the coarse mesh instead of the intersection with a higher finite element for ϕ_S (see figure 3) as proposed by Wheeler and Yotof in [19]. The interest of this version is to derive an a posteriori error estimate.

From (24), one can derive the discrete problem to solve. We give here the form of the discrete problem for two subdomains $\mathcal{R}_1$ and $\mathcal{R}_2$:

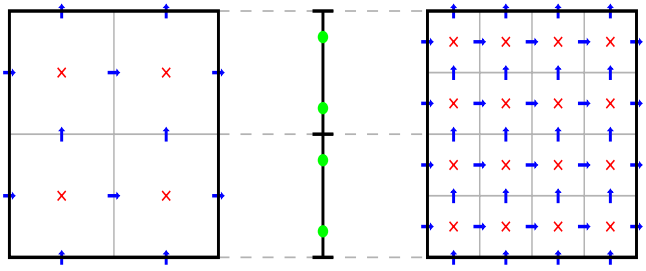

Fig. 3. Mesh of an interface proposed by Wheeler and Yotof in [19] for RT0 finite elements.

$$\begin{pmatrix} A_1 & B_1 & 0 & 0 & C_{1,2} \\ {}^TB_1 & T_1 & 0 & 0 & 0 \\ 0 & 0 & A_2 & B_2 & C_{2,1} \\ 0 & 0 & {}^TB_2 & T_2 & 0 \\ {}^TC_{1,2} & 0 & {}^TC_{2,1} & 0 & 0 \end{pmatrix} \begin{pmatrix} \boldsymbol{P}_1 \\ \Phi_1 \\ \boldsymbol{P}_2 \\ \Phi_2 \\ \Lambda_{1,2} \end{pmatrix} = \begin{pmatrix} 0 \\ S_{f_1} \\ 0 \\ S_{f_2} \\ 0 \end{pmatrix}. \tag{25}$$

For $n = 1, 2$, $\boldsymbol{P}_n$ (resp. Φ_n) is the discrete current (resp. flux) $\mathcal{R}_n$. $\Lambda_{1,2}$ is the discrete Lagrange multiplier on the interface between the subdomains 1 and 2. The matrices A_n (resp. B_n, T_n, $C_{1,2}$) are constructed from a (resp. b, t, l_S).

As the matrices T_n are diagonal due to the RTN finite element, one can easily remove the unknowns Φ_n from (25). We denote $W_n = A_n + B_n T_n^{-1\,T} B_n$, thus it stands:

$$\begin{pmatrix} W_1 & 0 & C_{1,2} \\ 0 & W_2 & C_{2,1} \\ {}^TC_{1,2} & {}^TC_{2,1} & 0 \end{pmatrix} \begin{pmatrix} \boldsymbol{P}_1 \\ \boldsymbol{P}_2 \\ \Lambda_{1,2} \end{pmatrix} = \begin{pmatrix} T_1^{-1}S_{f_1} \\ T_2^{-1}S_{f_2} \\ 0 \end{pmatrix}. \tag{26}$$

And we also have:

$$T_n\phi_n = {}^TB_n\boldsymbol{P}_n + S_{f_n} \tag{27}$$

From system (26), we derive a system only on $\Lambda_{1,2}$:

$$\left({}^TC_{1,2}W_1^{-1}C_{1,2} + {}^TC_{2,1}W_2^{-1}C_{2,1}\right)\Lambda_{1,2} = {}^TC_{1,2}W_1^{-1}T_1^{-1}S_{f_1} + {}^TC_{2,1}W_2^{-1}T_2^{-1}S_{f_2}. \tag{28}$$

One can notice that the matrix on the left hand side is positive definite symmetric, this can be solved by the gradient conjugate method which is parallelisable. Moreover the P_n can be computed at the same time.

III. THE SP$_N$ MULTIGROUP PROBLEM

To derive the SP$_N$ multigroup model one can suppose that the angular flux and the cross sections are piecewise constant over a discrete energy set and expand the angular flux over the spherical harmonics [20]. The new unknowns are denoted by $\underline{\phi}^g$ (resp. $\underline{\mathbf{p}}^g$) the vector containing the even (resp. odd) moments of the angular flux. Thus the equations read, for every energy group g:

Find $(\underline{\mathbf{p}}^g, \underline{\phi}^g, k_{\text{eff}})$, for all g in $\{1..G\}$, such that:

$$\left\{\begin{array}{rcll} (\mathbb{T}_o^g)^{-1}\underline{\mathbf{p}}^g + \mathbb{H}\mathbf{grad}\underline{\phi}^g &=& \displaystyle\sum_{g'\neq g} \mathbb{S}_o^{g'\to g}\underline{\mathbf{p}}^{g'} & \text{in } \mathcal{R}, \\ {}^t\mathbb{H}\text{div }\underline{\mathbf{p}}^g + \mathbb{S}_e^g\underline{\phi}^g &=& \displaystyle\sum_{g'\neq g} \mathbb{S}_e^{g'\to g}\underline{\phi}^{g'} & \\ & & \displaystyle+\frac{\chi^g}{k_{\text{eff}}}\sum_{g'}\mathbb{M}_f^{g'}\underline{\phi}^{g'} & \text{in } \mathcal{R}, \\ \underline{\phi}^g &=& 0 & \text{on } \partial\mathcal{R}. \end{array}\right. \tag{29}$$

In the previous equations, the unknowns are vectors where each component is an harmonic. The matrices Σ are the diagonal matrices formed by the moments of the corresponding cross sections. The link between odd and even moments is done by the matrix $\mathbb{H}$ which is an upper bidiagonal matrix with only ones.

In order to extend the previous results to this model, one has to consider the one-speed SP_N problem, which reads:
Find $(\underline{\mathbf{p}}, \underline{\phi})$, for every source $(S_{\boldsymbol{p}} S_\phi)$, such that:

$$\left\{\begin{array}{rcll} D^{-1}\underline{\mathbf{p}} + \mathbb{H}\mathbf{grad}\underline{\phi} &=& S_{\boldsymbol{p}} & \text{in } \mathcal{R}, \\ {}^t\mathbb{H}\text{div }\underline{\mathbf{p}} + \Sigma_a\underline{\phi} &=& S_\phi & \text{in } \mathcal{R}, \\ \underline{\phi}^g &=& 0 & \text{on } \partial\mathcal{R}. \end{array}\right. \tag{30}$$

The theory done for the diffusion case works in this case as long as the diagonal matrix operators D and σ_a satisfy the same regularity as for the diffusion case. The inf-sup condition holds thanks to the coercivity of the matrix $\mathbb{H}$. Indeed, one can easily prove that, there exists $\alpha > 0$ such that, for all $\boldsymbol{x}$ in $\mathbb{R}^d$:

$$(\mathbb{H}\boldsymbol{x}|\boldsymbol{x}) \geq \alpha\|x\|^2 \tag{31}$$

Moreover, as the adjoint problem is the source problem with only a source on the second equation, the Aubin-Nitsche-type estimate still holds. Thus, we have the same result on the monospeed model as on the diffusion model.

In order to consider the energy dependence we have to make the following assumption: the nuclear fissions emit only neutrons in the first energy group. Under this assumption, two cases appear. In the case of no up-scattering, one can use the Gauss algorithm to rewrite equation (29) with the form of (30) with $S_{\boldsymbol{p}}$ and S_ϕ depending only on the first group unknowns $(\boldsymbol{p}^1, \phi^1)$ and the criticality k_{eff}.

In the other case, one can decomposed the problem to use the case without up-scattering. One can rewrite (29) with one operator, thus it stands:

$$\mathbb{A}\begin{pmatrix} (\boldsymbol{p}^1, \phi^1) \\ \vdots \\ (\boldsymbol{p}^G, \phi^G) \end{pmatrix} = \begin{pmatrix} (0, \dfrac{\chi^1}{k_{\text{eff}}}\displaystyle\sum_{g'}\nu^{g'}\Sigma_f^{g'}\phi^{g'}) \\ 0 \\ 0 \end{pmatrix}. \tag{32}$$

The operator $\mathbb{A}$ can be decomposed as $\mathbb{A} = \mathbb{L}+\mathbb{U}$ such that $\mathbb{L}$ is a triangular inferior operator and $\mathbb{U}$ is strictly triangular superior operator. The problem is still wellposed if one is not a eigenvalue of $\mathbb{L}^{-1}\mathbb{U}$.

IV. RESULTS

We first verify the convergence rate for a conforming mesh without DDM. Then we present results with a conforming mesh and the DDM for a nuclear reactor. We finish with an illustration of a non-conforming mesh.

1. Verification of the Convergence Rate

We adapt the benchmark described in [6, 21]. The problem can be written as:

$$\left\{\begin{array}{rcll} D^{-1}\mathbf{p} + \mathbf{grad}\phi &=& 0 & \text{in } \mathcal{R}, \\ \text{div }\mathbf{p} + \phi &=& \frac{1}{k_{\text{eff}}}\phi & \text{in } \mathcal{R}, \\ \phi &=& 0 & \text{on } \partial\mathcal{R}. \end{array}\right. \tag{33}$$

Coefficient D is taken piecewise constant as shown on figure 4.

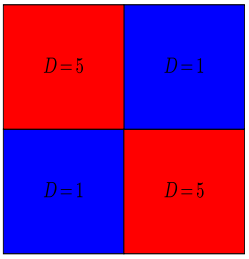

Fig. 4. Geometry for a discontinuous coefficient case.

In this case we do not know the analytic solution. Thus, to obtain the convergence rate, we use the k_{eff} computed on a fine mesh. The obtained value is $k_{\text{eff}} \simeq 0.99512708$.

For problem (33) it is known that the first eigenfunction is regular. Thus we expect a convergence rate of 2 with RT0 FEM.

In table I, we show, for different numbers of degrees of freedom N, the number of power iterations N_{iter}, the k_{eff}^h computed, the error on the k_{eff} in pcm (10^{-5}) and the experimental convergence rate of the method τ for the eigenvalue. All resolutions are done on uniform meshes with only squares.

N	N_{iter}	k_{eff}^h	$\lvert k_{\text{eff}} - k_{\text{eff}}^h\rvert/k_{\text{eff}}$	$\tau_{k_{\text{eff}}}$
16	63	0.99451405	$6.16e^{+1}$	
56	95	0.99488991	$2.38e^{+1}$	1.37
208	91	0.99506205	$6.53e^{+0}$	1.87
800	107	0.99511045	$1.67e^{+0}$	1.97
3 134	113	0.99512291	$4.19e^{-1}$	1.99
12 416	111	0.99512601	$1.08e^{-1}$	1.96
49 408	115	0.99512678	$2.99e^{-2}$	1.85

TABLE I. Results for problem (33) with different meshes.

The experimental convergence rate is near 2 as we expected.

The strange behaviour of the convergence rate for the finest mesh comes from the machine epsilon. The computations are done with single precision, thus, for the finest mesh the error is near to the machine epsilon.

2. DDM for a large heavy steel reactor

Here we illustrate the DDM on a large heavy steel reactor described in figure 5. The computations are done with two groups of energy and with the diffusion model. The conforming meshes used has 115 309 cells.

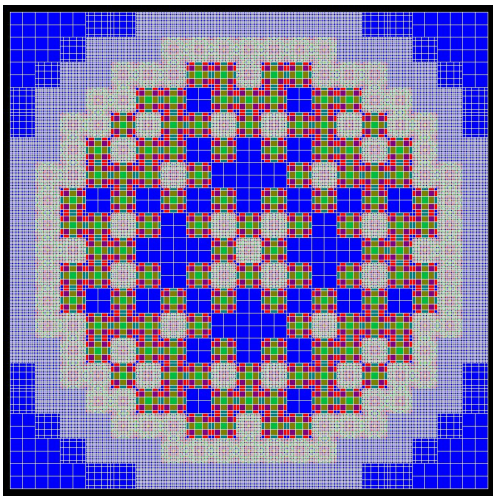

Fig. 5. Geometry of a large heavy steel reactor.

In table II, we present the number of power iterations N_{iter}, the criticity computed k^h_{eff}, the error in pcm and the computational time in second for different number of domains.

DD	N_{iter}	k^h_{eff}	$\lvert k_{\text{eff}} - k^h_{\text{eff}}\rvert / k_{\text{eff}}$	Time
1×1	114	1.15941	24.73	1.25
2×2	121	1.15940	24.55	3.25
5×5	119	1.15940	24.59	4.71
10×10	116	1.15940	24.67	6.83
19×19	114	1.15941	24.73	13.54

TABLE II. Results for several numbers of domains for a large heavy steel reactor.

With this DDM the number of power iterations stay closed to the one without DDM. This fact comes from the use of the gradient conjugate method to solve the problem on the Lagrange multiplier. Moreover this DDM does not deteriorate the computation precision.

As the method is not parallelised yet, the time cost of the DDM increases as the number of domains increases. But if we look at the time by domain, with a perfect parallelisation, one can obtain a decrease of the computation time for the same precision.

3. Resolution with a Non-Conforming Mesh

In this case we evaluate the criticity for a simple reactor given in figure 6. We use the DDM to compute the flux on the mesh of the geometry. Each assembly is a domain with is own mesh.

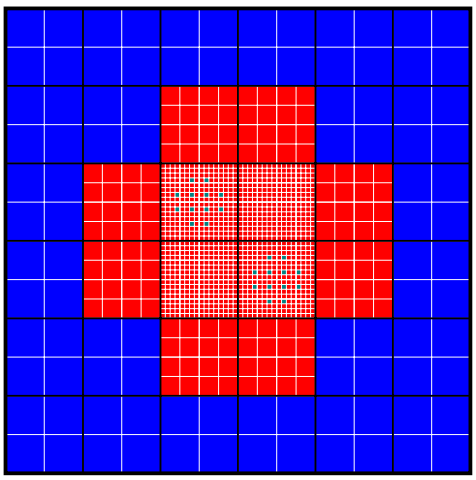

Fig. 6. Geometry for a discontinuous coefficient case.

In table III, we show results for different meshes. The first line and the last one correspond to conforming mesh derived from the geometry. In the second and third lines we used the non-conforming mesh described by the assemblies. The difference between this to computation is the number of power iterations. Indeed, in the first one we stop at the same number as the conforming mesh. Whereas in the second case we stop when the convergence criterium was satisfy. The columns in table III correspond to the number of cells N, the number of power iterations N_{iter}, k^h_{eff} computed, the error in pcm on the eigenvalue and the computational time in second.

The conforming mesh derived from this geometry has 1 936 cells while the mesh of the geometry has only 1 248 cells. Moreover the precision is nearly the same between the conforming and non-conforming mesh. Thus one can conclude that the use of the non-conforming is a way to reduce memory cost for the same precision. But the computation time is nearly double between this two meshes. This can be improved by parallelised the method.

V. CONCLUSIONS AND PERSPECTIVES

In this work we studied some diffusion like models of a nuclear core. Those models are the SP_1/diffusion case and the multigroup SP_N one. We studied them to ensure that they have good mathematical properties as the well-posedness and the convergence. Then we developed a non-conforming DDM with Lagrange multiplier. We confirmed the theory and the use of non-conforming mesh with two numerical tests. The method can still be improved by an a posteriori error estimate to adapt the mesh to each iteration of the power inverse algorithm [22]. For singular solution one can also use singular complement method as it exists in electromagnetism [23].

	N	N_{iter}	k^h_{eff}	$\lvert k_{\text{eff}} - k^h_{\text{eff}}\rvert / k_{\text{eff}}$	Time
Conforming	1 936	75	1.23589	5.60	1.29
Non-conforming	1 248	75	1.23603	5.77	2.27
Non-conforming	1 248	97	1.23602	4.69	3.09
Reference	193 600		1.23596		

TABLE III. Comparison between non-conforming and uniform refinement for problem (33)

VI. ACKNOWLEDGEMENTS

We gratefully acknowledge EDF for its long time partnership and the support.

REFERENCES

1. M. G. KREIN and M. A. RUTMAN, "Linear Operators Leaving Invariant a Cone in a Banach Space," *Am. Math. Soc. Transl.*, **26**, 199–325 (1950).
2. A. M. BAUDRON and J. LAUTARD, "MINOS: A Simplified Pn Solver for Core Calculation," *Nucl. Sci. Eng.*, **155**, *2*, 250–263 (Feb. 2007).
3. E. JAMELOT, A. M. BAUDRON, and J. J. LAUTARD, "Domain Decomposition for the SP_NSolver MINOS," *Transp. Theory Stat. Phys.*, **41**, *7*, 495–512 (2012).
4. E. JAMELOT, P. CIARLET, JR., A. M. BAUDRON, and J. J. LAUTARD, "Domain Decomposition for the Neutron SP_N Equations," in "Domain Decomposition Methods in Science and Engineering XXI," Springer (2012), Lecture Notes in Computational Science and Engineering, pp. 677–685.
5. E. JAMELOT and P. CIARLET, JR., "Fast Non-Overlapping Schwarz Domain Decomposition Methods for Solving the Neutron Diffusion Equation," *J. Comput. Phys.*, **241**, 445–463 (2013).
6. M. COSTABEL, M. DAUGE, and S. NICAISE, "Singularities of Electromagnetic Fields in Polyhedral Domains," *M2AN Math Model Numer Anal*, **33**, *3*, 627–649 (1999).
7. B. I. WOHLMUTH, *Discretization Methods and Iterative Solvers Based on Domain Decomposition*, *Lecture Notes in Computational Science and Engineering*, vol. 17, Springer-Verlag (2001).
8. P. CIARLET, JR., E. JAMELOT, and F. KPADONOU, "Domain Decomposition Methods for the Diffusion Equation with Low-Regularity Solution," *Submitt. CAMWA* (2017).
9. I. BABUŠKA, "Error-Bounds for Finite Element Method," *Numer. Math.*, pp. 322–33 (1971).
10. D. SCHNEIDER, *Éléments Finis Mixte Duaux Pour La Résolution Numérique de l'Équation de La Diffusion Neutronique En Géométrie Hexagonale*, Ph.D. thesis, UPMC (2000).
11. P. A. RAVIART and J. M. THOMAS, "A Mixed Finite Element Method for 2-Nd Order Elliptic Problems," in "Mathematical Aspects of Finite Element Methods," Springer, Rome (1975), *Lecture Notes in Mathematics*, vol. 606, pp. 292–315.
12. J. C. NÉDÉLEC, "Mixed Finite Elements in $\mathbb{R}3$," *Numer. Math.*, **35**, *3*, 315–341 (Sep. 1980).
13. A. ERN and J. L. GUERMOND, *Theory and Pratice of Finite Elements*, Springer (2004).
14. A. BERMÚDEZ, P. GAMALLO, M. R. NOGUEIRAS, and R. RODRÍGUEZ, "Approximation Properties of Lowest-Order Hexahedral Raviart–Thomas Finite Elements," *Comptes Rendus Académie Sci. Paris Ser. I*, **340**, 687–692 (2005).
15. R. S. FALK and J. E. OSBORN, "Error Estimates for Mixed Methods," *RAIRO Anal Numer*, **14**, 249–277 (1980).
16. P. CIARLET, JR., L. GIRET, E. JAMELOT, and F. KPADONOU, "Numerical Analysis of the Mixed Finite Element Method for the Neutron Diffusion Eigenvalue Problem," *Prog.* (2017).
17. J. E. OSBORN, "Spectral Approximation for Compact Operators," *Math Comp*, **29**, 712–725 (1975).
18. D. BOFFI, D. GALLISTL, F. GARDINI, and L. GASTALDI, "Optimal Convergence of Adaptive FEM for Eigenvalue Clusters in Mixed Form," (2015).
19. M. F. WHEELER and I. YOTOV, "A Posteriori Error Estimates for the Mortar Mixed Finite Element Method," *SIAM J. Numer. Anal.*, **43**, *3*, 1021–1042 (2005).
20. G. POMRANING, "Asymptotic and Variational Derivations of the Simplified P_N Equations," *Ann. Nucl. Energy*, **20**, 623–637 (1993).
21. M. DAUGE, P. FRAUENFELDER, and M. DURUFLÉ, "Benchmark Computations for Maxwell Equations for the Approximation of Highly Singular Solutions," https://perso.univ-rennes1.fr/monique.dauge/core/index.html (2004).
22. M. VOHRALIK, "A Posteriori Error Estimates for Lowest-Order Mixed Finite Element Discretization of Convection-Diffusion-Reaction Equations," *SIAM J. Numer. Anal.*, **45**, *4*, 1570–1599 (2007).
23. F. ASSOUS, P. CIARLET, JR., and SONNENDRÜCKER, "Resolution of the Maxwell Equations in a Domain with Reentrant Corners," *Math. Model. Numer. Anal.*, **32**, 359–389 (1998).